Clinical Imaging 53 (2019) 143–150

Contents lists available at ScienceDirect

Clinical Imaging

journal homepage: www.elsevier.com/locate/clinimag

Body Imaging

Clinical utility of susceptibility-weighted MR sequence for the evaluation of uterine sarcomas☆

Mayumi Takeuchi[a,*], Kenji Matsuzaki[b], Masafumi Harada[a]

[a] Department of Radiology, Tokushima University, 3-18-15, Kuramoto-cho, Tokushima 7708503, Japan
[b] Department of Radiological Technology, Tokushima Bunri University, 1314-1, Shido, Sanuki-city, Kagawa 7692193, Japan

ARTICLE INFO

Keywords:
Magnetic resonance imaging (MRI)
Susceptibility-weighted magnetic resonance sequence
T2 star-weighted angiography (SWAN)
Uterus
Sarcoma

ABSTRACT

Purpose: High intensity intra-tumoral hemorrhagic necrosis on T1-weighted images is a suggestive finding for uterine sarcomas, however, the reported prevalence varies. The purpose of this study is to evaluate the capability of susceptibility-weighted MR sequences (SWS) for the diagnosis of uterine sarcomas.
Materials and methods: MR imaging of surgically proven 10 uterine sarcomas and 24 benign leiomyomas were retrospectively evaluated for the presence of high intensity areas on T1-weighted images and signal voids on SWS (T2 star-weighted angiography: SWAN).
Results: High intensity areas on T1-weighted images and signal voids on SWS were observed in 40% and 100% of sarcomas, whereas 0% and 4% of leiomyomas, respectively. The accuracy, sensitivity, and specificity for T1-weighted images were 82%, 40%, and 100%, and for SWS were 97%, 100%, and 96%, respectively.
Conclusion: The demonstration of intra-tumoral hemorrhage in patients suspected with uterine sarcomas by SWS may provide valuable diagnostic findings.

1. Introduction

Uterine sarcomas are uncommon heterogeneous group of tumors of mesenchymal, epithelial, or mixed epithelial-mesenchymal origin, and recently show increased incidence possibly due to increase in aging population [1]. Uterine sarcomas may originate from smooth muscle in myometrium (leiomyosarcoma), from endometrial stroma (endometrial stromal sarcoma) or both (adenosarcoma). Whereas, carcinosarcoma is the most common subtype of uterine sarcomas and recently is regarded as a subset of endometrial carcinoma with sarcomatous differentiation. Because the clinical course of uterine sarcomas is usually aggressive with poor prognosis, it should be correctly diagnosed for the appropriate surgical management and adjuvant therapy. Since the uterine body is situated deep in the female pelvis, biopsy is not commonly performed for uterine myometrial tumors and preoperative assessment based on magnetic resonance (MR) imaging is required. Various imaging characteristics of uterine sarcomas have been reported based on the morphological appearances, and intra-tumoral necrosis and hemorrhage are suggestive findings for sarcomas [1–6]. However, both degenerated areas in benign leiomyomas and necrotic areas in sarcomas may appear as unenhanced areas on post-contrast images [1,4,7]. Intra-tumoral hemorrhage may appear as high intensity areas on T1-weighted images, however, the reported prevalence varies (18–68%) possibly because only methemoglobin in subacute hemorrhage may show high signal intensity [2,3,5,6,8,9]. Susceptibility-weighted MR sequences such as SWI (Susceptibility-weighted imaging) or SWAN (T2 star-weighted MR angiography) are MR techniques which maximize sensitivity to susceptibility effects, and have exquisite sensitivity to blood products such as deoxyhemoglobin and hemosiderin resulting from acute and chronic hemorrhage, respectively [10–13]. SWAN uses multiple magnitude images with different echo times for the image generation. SWAN applies a multi-TE readout technique with high signal-to-noise-ratio and helps clearly delineate small vessels and microbleeds [11].

On the other hand, the usefulness of diffusion-weighted imaging (DWI) in differentiating uterine sarcomas from benign leiomyomas has been reported [14–17]. The uterine sarcomas showed high signal intensity on DWI ($b = 800–1000\ s/mm^2$) and low apparent diffusion coefficient (ADC) values (cut-off value: 1.05 to $1.23 \times 10^{-3}\ mm^2/s$.) [14–17]. However, there were considerable overlaps in ADC values between sarcomas and leiomyomas possibly due to high cellularity of sarcomas and cellular leiomyomas, and fibrous components of usual leiomyomas. In addition, some leiomyomas may also show high signal intensity on DWI reflecting T2 shine-through effect due to edema or

☆ Declarations of interest: none.

* Corresponding author.
E-mail addresses: mayumi@tokushima-u.ac.jp (M. Takeuchi), kenji@kgw.bunri-u.ac.jp (K. Matsuzaki), masafumi@tokushima-u.ac.jp (M. Harada).

https://doi.org/10.1016/j.clinimag.2018.10.015
Received 18 June 2018; Received in revised form 13 September 2018; Accepted 12 October 2018

Table 1
Summary of cases with uterine sarcomas.

Case no.	Age (years)	Lesion no.	Pathological diagnosis	Size (mm)	T1WI high	SWAN signal voids	T2WI	DWI	ADC ($\times 10^{-3}$ mm^2/s)
1	57	1	Leiomyosarcoma	70	+	+	High	High	0.48
2	59	2	Endometrial Stromal sarcoma	140	+	+	High	High	0.83
3	76	3	Carcinosarcoma	86	−	+	High	High	0.91
4	48	4	Carcinosarcoma	45	−	+	High	High	0.92
5	59	5	Carcinosarcoma	49	−	+	High	High	0.86
6	40	6	Carcinosarcoma	100	−	+	High	High	0.72
7	58	7	Carcinosarcoma	132	+	+	High	High	0.71
8	75	8	Carcinosarcoma	61	−	+	High	High	1.03
9	53	9	Leiomyosarcoma	131	−	+	High	High	0.94
10	74	10	Leiomyosarcoma	136	+	+	High	High	0.94

SWAN, T2 star-weighted angiography; ADC, apparent diffusion coefficient.

Table 2
Summary of cases with leiomyomas.

Case no.	Age (years)	Lesion no.	Pathological diagnosis	Size (mm)	T1WI high	SWAN signal voids	T2WI	DWI	ADC ($\times 10^{-3}$ mm^2/s)
1	55	1	Usual	40	–	–	Low	Low	1.09
		2	Usual	40	–	–	Low	Low	1.02
2	54	3	Cellular	83	–	+	High	High	1.11
3	57	4	Usual	62	–	–	Low	High	0.86
4	41	5	Usual	47	–	–	Low	Low	1.04
5	63	6	Usual	181	–	–	Low	Low	1.23
6	50	7	Usual	107	–	–	Low	Low	1.03
		8	Usual	117	–	–	Low	Low	1.34
		9	Usual	41	–	–	Low	Low	1.29
		10	Usual	54	–	–	Low	Low	0.97
		11	Usual	46	–	–	Low	Low	1.05
		12	Usual	50	–	–	Low	Low	1.08
		13	Usual	47	–	–	Low	Low	1.39
7	41	14	Usual	154	–	–	Low	Low	1.23
8	49	15	Usual	61	–	–	High	Low	1.36
9	43	16	Usual	73	–	–	Low	Low	0.97
		17	Usual	41	–	–	Low	Low	1.06
10	48	18	Usual	82	–	–	Low	Low	1.12
		19	Usual	52	–	–	Low	Low	1.26
		20	Usual	48	–	–	Low	Low	1.35
11	36	21	Usual	57	–	–	Low	Low	0.94
12	37	22	Usual	72	–	–	Low	Low	1.29
13	55	23	Usual	46	–	–	Low	Low	1.25
		24	Usual	88	–	–	High	High	1.83

SWAN, T2 star-weighted angiography; ADC, apparent diffusion coefficient.

degeneration [14,15]. Most of uterine smooth muscle tumors are usual (ordinary) leiomyomas, and leiomyosarcomas are rare. In between benign usual leiomyomas and malignant leiomyosarcomas, there are several leiomyoma variants such as cellular, mitotically active, and atypical leiomyomas, as well as smooth muscle tumors of uncertain malignant potential (STUMP) [18]. Such leiomyoma variants are uncommon (about 1 in 100 cases with a uterine mass presumed to be a leiomyoma), and leiomyosarcomas are quite rare (about 1 in 500 cases) [18].

The purpose of this study was to evaluate the capability of susceptibility-weighted MR sequence (SWAN) in detecting the signal voids due to hemorrhagic necrosis and the added value for the diagnosis of uterine sarcomas.

2. Materials and methods

2.1. Patients

The institutional review board in our hospital approved this retrospective study, and waived the requirement for written informed consent of patients. We cross-referenced the database of the Department of Obstetrics and Gynecology to identify all patients with pathologically proven uterine sarcomas who had undergone MRI examinations including SWAN between April 2012 and May 2017. A total of 10 women with a mean age of 60 years (range, 40–76 years) who met the criteria were included in the current study (Table 1). 10 sarcomas included six carcinosarcomas, three leiomyosarcomas, and one endometrial stromal sarcoma. The median lesion size, which was the longest diameter measured by MR imaging was 86 mm (range, 45–140 mm). 24 surgically proven benign leiomyomas (≥ 40 mm) in 13 women with a mean age of 48 years (range, 36–63 years) who had undergone MRI examinations including SWAN were randomly selected during the same period as a comparison group. 23 usual leiomyomas with/without degeneration and one cellular leiomyoma were included. The median lesion size was 56 mm (range, 40–181 mm) (Table 2).

2.2. MR imaging

Fast spin-echo T2-weighted images (TR/TE, 5000–5500/94.9–111.7 ms), gradient-echo T1-weighted images with fat-saturation (fast spoiled gradient-recalled echo, TR/TE, 3.9–4.6/1.7–2.1 ms), DWI (TR/TE, 4000/51–56.2 ms; b = 0 and 800 s/mm^2), and SWAN (three-dimensional multi-echo gradient echo, TR/TE, 41.8–43.0/27.0–27.4 milliseconds; matrix size, 320 × 192–256; field of view, 28 × 28 cm;

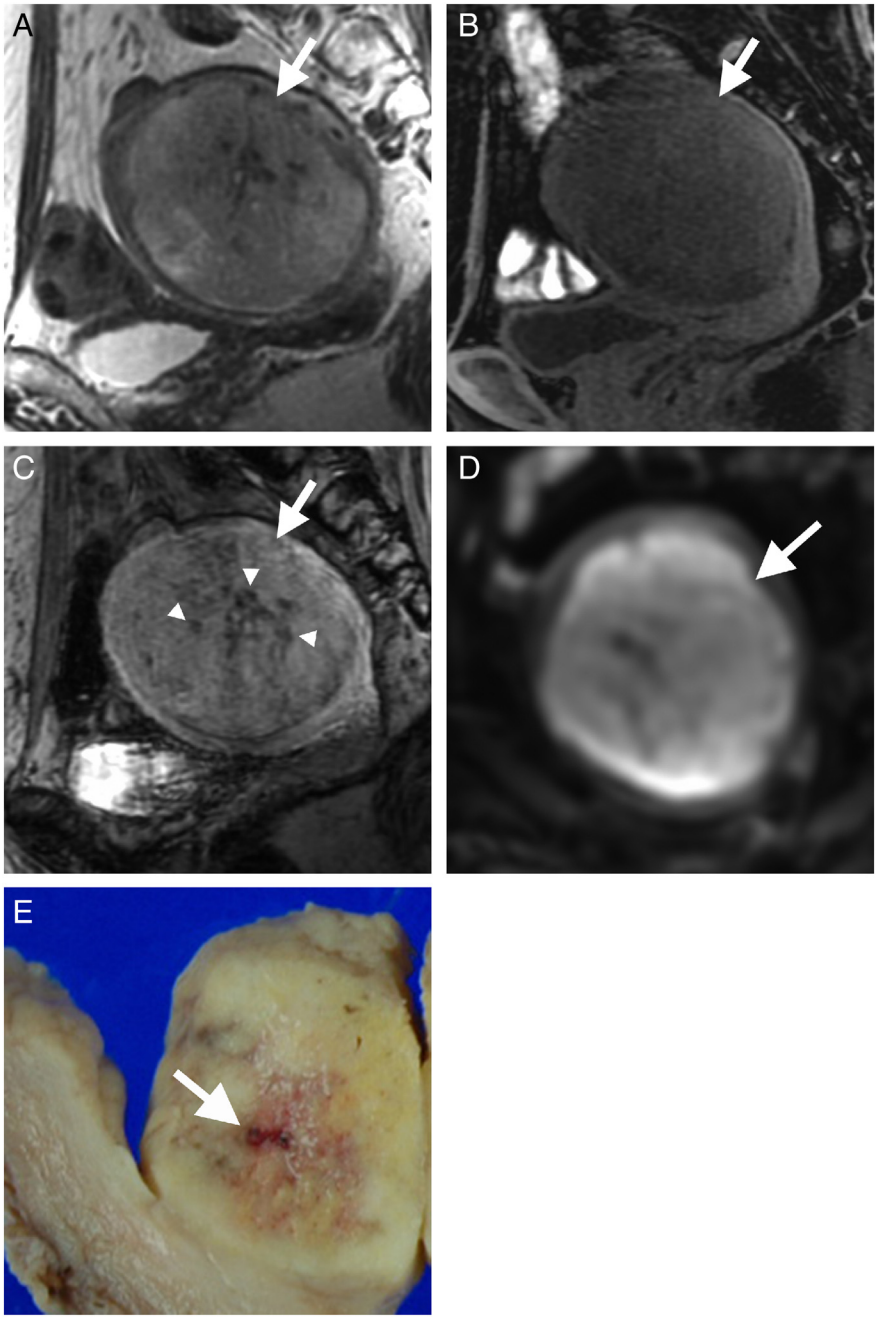

Fig. 1. A 76-year-old woman with carcinosarcoma (Sarcoma_Case 3_Lesion 3). A. Sagittal T2-weighted image shows a large, heterogeneous uterine corpus mass (arrow). B. No high intensity area is observed within the mass (arrow) on sagittal fat-saturated T1-weighted image. C. Spotty signal voids (arrowheads) are scattered within the mass (arrow) on sagittal SWAN. D. The mass (arrow) shows heterogeneous high intensity on DWI. E. Spotty intra-tumoral hemorrhagic foci (arrow) are revealed on the cut surface of the mass.

section thickness, 3–5 mm; spacing, 1.5–2.5 mm) were obtained for all patients with 3-T superconducting MRI system (Discovery MR750, GE Healthcare, Waukesha, WI, USA) with 32-channel body-array torso coils.

2.3. Analysis methods

Two radiologists with 27 and 18 years of experience in gynecological MRI qualitatively evaluated the images for the presence of high signal intensity foci on fat-saturated T1-weighted images, and of signal voids on SWAN within the masses. Signal voids due to calcification on SWAN were excluded by referring computed tomography (CT) images, or phase images obtained together with magnitude images of SWAN. Curvilinear tortuous flow voids reflecting the feeding arteries were also excluded. Signal intensities of the lesions on DWI and on T2-weighted images were visually evaluated and classified as high (high intensity compared to the myometrium) or low (iso to low intensity compared to the myometrium). The reviewers examined all images of the cases independently and then resolved discrepancies by consensus. After the evaluation, accuracy, sensitivity, and specificity were computed for different sequences.

The mean ADC values ($\times 10^{-3}$ mm^2/s) were measured in a circular region of interest (ROI) in one representative region within the lesions from ADC maps on the workstation (AW4.2, General Electric, Milwaukee, WI). The ROI was placed on solid tumoral component for heterogeneous lesions so as not to contain necrotic cysts as much as

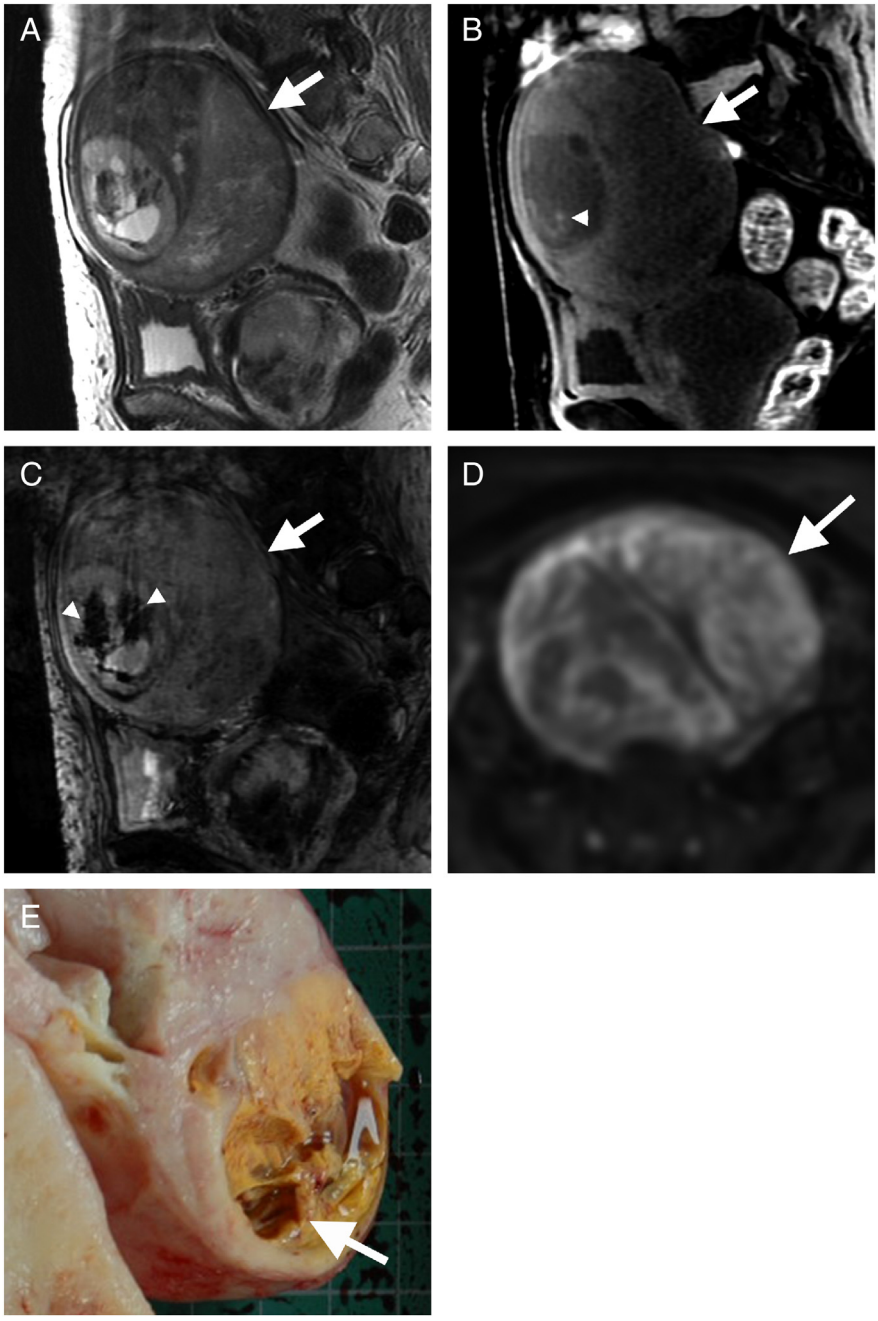

Fig. 2. A 59-year-old woman with endometrial stromal sarcoma (Sarcoma_Case 2_Lesion 2). A. Sagittal T2-weighted image shows a large, heterogeneous uterine corpus mass (arrow). B. Small high intensity areas (arrowhead) are observed within the mass (arrow) on sagittal fat-saturated T1-weighted image. C. Signal voids (arrowheads) are prominent within the mass (arrow) on sagittal SWAN. D. The mass (arrow) shows heterogeneous high intensity on DWI. E. Intra-tumoral hemorrhagic necrosis (arrow) is revealed on the cut surface of the mass.

possible by referring T2-weighted images. The ROI was placed so as not to contain high intensity areas on T1-weighted images or signal voids on SWAN for avoiding susceptibility effect of hemorrhagic contents.

2.4. Statistical analysis

Statistical analysis was performed using Excel for Mac 2011 (Microsoft, Seattle, WA) with the add-in software Statcel 3 (OMS, Tokyo, Japan). Mann-Whitney *U* test was used to compare ADCs between sarcomas and benign leiomyomas. Values of $P < 0.05$ were considered statistically significant.

3. Results

High signal intensity foci on fat-saturated T1-weighted images were detected in four of ten sarcomas (40%), whereas signal voids on SWAN were detected in all sarcomas (100%) (Figs. 1, 2). No high signal intensity foci on fat-saturated T1-weighted images were observed in all 24 leiomyomas, and signal voids on SWAN were observed in only one leiomyoma (4%) (Figs. 3, 4). The leiomyoma with hemorrhagic foci was histologically diagnosed as cellular leiomyoma (Fig. 3). The accuracy, sensitivity, and specificity for T1-weighted images were 82%, 40%, and 100%, and for SWAN were 97%, 100%, and 96%, respectively. The positive predictive value (PPV), negative predictive value (NPV), positive likelihood ratio (LR+), and negative likelihood ratio (LR−) for

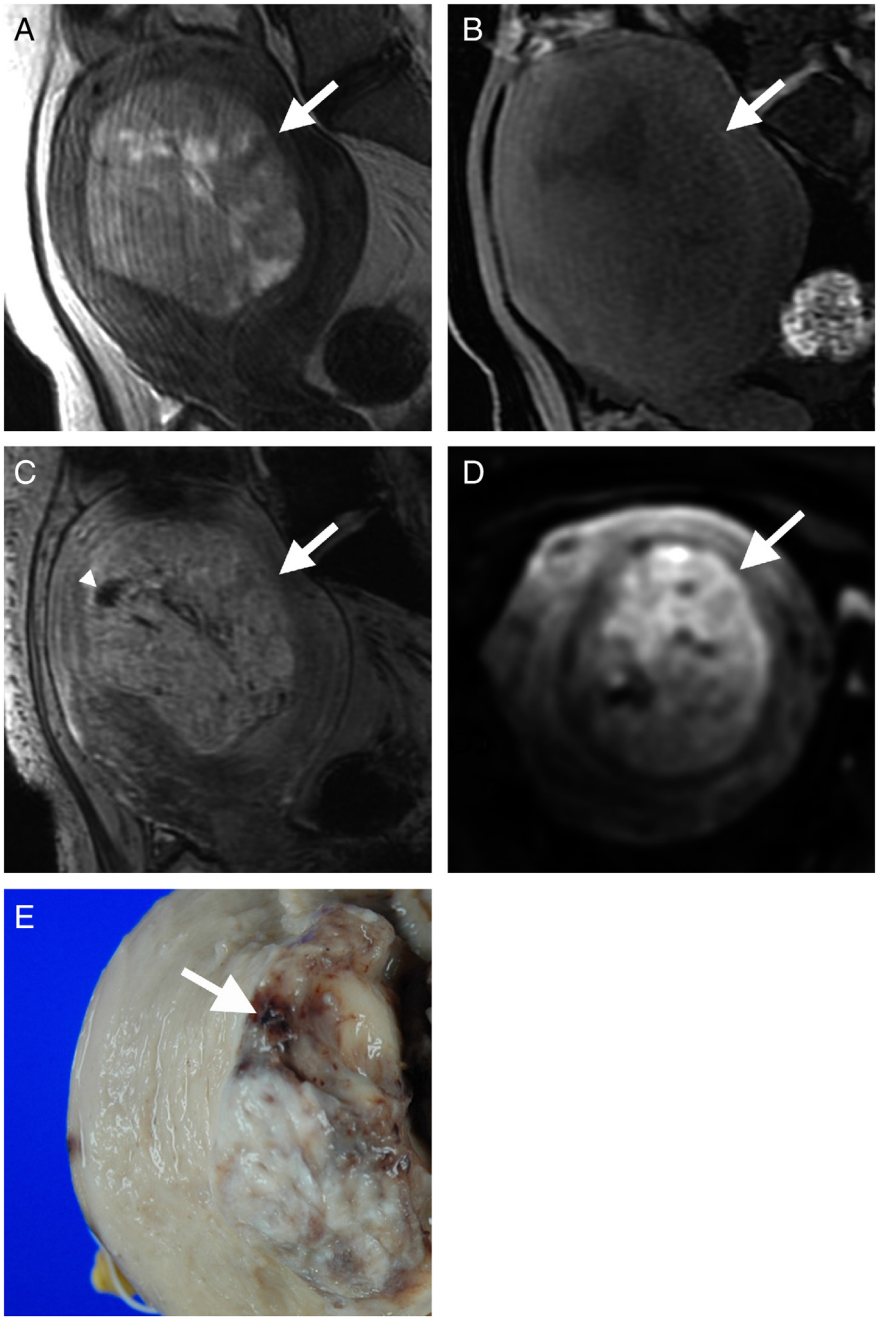

Fig. 3. A 54-year-old woman with cellular leiomyoma (Leiomyoma_Case 2_Lesion 3). A. Sagittal T2-weighted image shows a large, heterogeneous uterine corpus mass (arrow). B. No high intensity area is observed within the mass (arrow) on sagittal fat-saturated T1-weighted image. C. Speckled signal voids (arrowheads) are observed within the mass (arrow) on sagittal SWAN. D. The mass (arrow) shows heterogeneous high intensity on DWI. E. Intra-tumoral hemorrhagic foci (arrow) are revealed on the cut surface of the mass.

T1-weighted images were 100%, 80%, $+\infty$, and 0.6, and for SWAN were 91%, 100%, 25, and 0, respectively.

Concordance rates between two readers were excellent (kappa = 1.0 for SWAN) and good (kappa = 0.84 for T1-weighted images). One of the two reviewers pointed out small spotty high intensity foci in a carcinosarcoma on fat-saturated T1-weighted images considered as intra-tumoral hemorrhage, and the reviewers concluded that the high intensity foci were artifacts after the careful discussion.

All 10 sarcomas showed heterogeneous high signal intensity on DWI and T2-weighted images, whereas two leiomyomas (one cellular leiomyoma and one usual leiomyoma) also showed high signal intensity on DWI and T2-weighted images. One usual leiomyoma showed high signal intensity on DWI and low signal intensity on T2-weighted images, and one usual leiomyoma showed low signal intensity on DWI and high signal intensity on T2-weighted images. The other 20 usual leiomyomas showed low signal intensity both on DWI and T2-weighted images. Concordance rates between two readers were excellent (kappa = 1.0 for DWI and T2-weighted images).

The mean (SD) ADCs in the 10 sarcomas and in the 24 leiomyomas were 0.83 (0.16) $\times 10^{-3}$ mm^2/s and 1.17 (0.21) $\times 10^{-3}$ mm^2/s, respectively. There was significant difference (P = 0.00004) between the ADC in the sarcomas and that in the leiomyomas, however, there were several overlaps in the ADC values between sarcomas and benign leiomyomas (Fig. 5). Using a cutoff ADC value of 0.97 $\times 10^{-3}$ mm^2/s for uterine sarcomas resulted in a sensitivity of 91.7%, specificity of 90%, and accuracy of 91.2%.

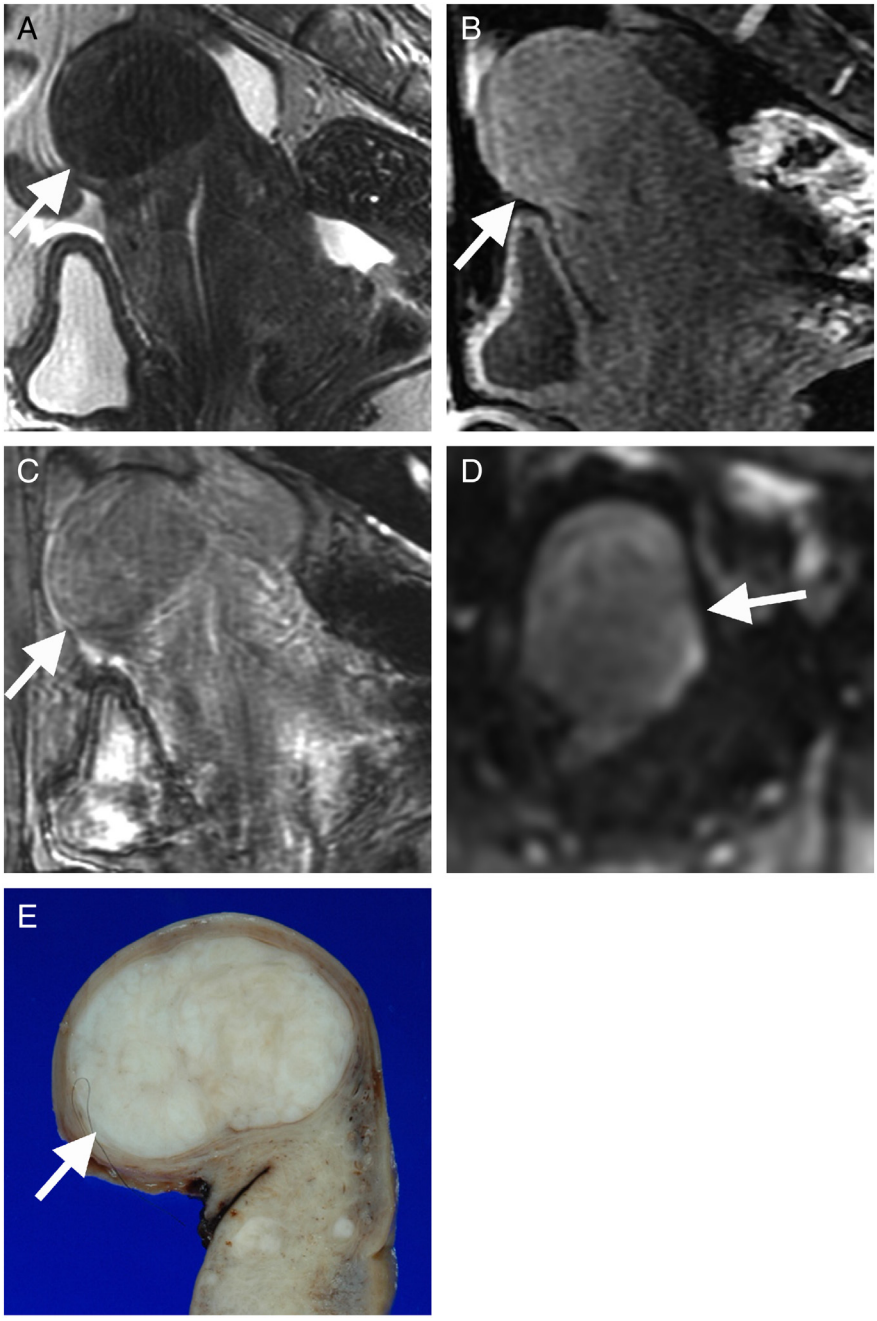

Fig. 4. A 55-year-old woman with usual leiomyoma (Leiomyoma_Case 13_Lesion 1). A. Sagittal T2-weighted image shows a low intensity uterine corpus mass (arrow). B. No high intensity area is observed within the mass (arrow) on sagittal fat-saturated T1-weighted image. C. No signal voids are observed within the mass (arrow) on sagittal SWAN. D. The mass (arrow) shows low intensity on DWI. E. No intra-tumoral hemorrhagic foci are observed on the cut surface of the mass.

4. Discussion

Intra-tumoral hemorrhage is often observed in sarcomas with coagulative necrosis due to the breakdown of tumor vasculature as hemorrhagic necrosis. The presence of high intensity areas on T1-weighted images may be characteristic for intra-tumoral hemorrhage, although the reported prevalence varies (18 to 68%) [2,3,5,6]. In our study only 40% of sarcomas showed high intensity areas on fat-saturated T1-weighted images, whereas all lesions revealed signal voids on susceptibility-weighted MR sequences (SWAN). That may be because high signal intensity on T1-weighted images due to the T1 shortening effect of methemoglobin may reflect only subacute hemorrhage, whereas signal voids on susceptibility-weighted MR sequences may reflect all phases of hemorrhage, especially both deoxyhemoglobin in acute phase and hemosiderin in chronic phase [8–13].

Sehgal et al. reported that susceptibility-weighted MR sequences (SWI) visualized blood products in high-grade brain tumors and improved tumor characterization than T1-weighted images. Because high-grade, aggressive tumors tend to have rapidly growing vasculature and multiple microhemorrhage or hemorrhagic necrosis may occur, detecting hemorrhagic areas within tumors could lead to improved determination of tumor status. In their report, SWI gave better information than T1WI (in 71% of cases) in the evaluation of blood products in brain tumors [12]. Takeuchi et al. reported that high intensity hemorrhagic foci on fat-saturated T1-weighted images were detected in 50% of extra-ovarian endometriosis, whereas signal voids on susceptibility-weighted MR sequences (SWI) were detected in all lesions (100%), and concluded that SWI may improve the diagnostic ability of extra-ovarian

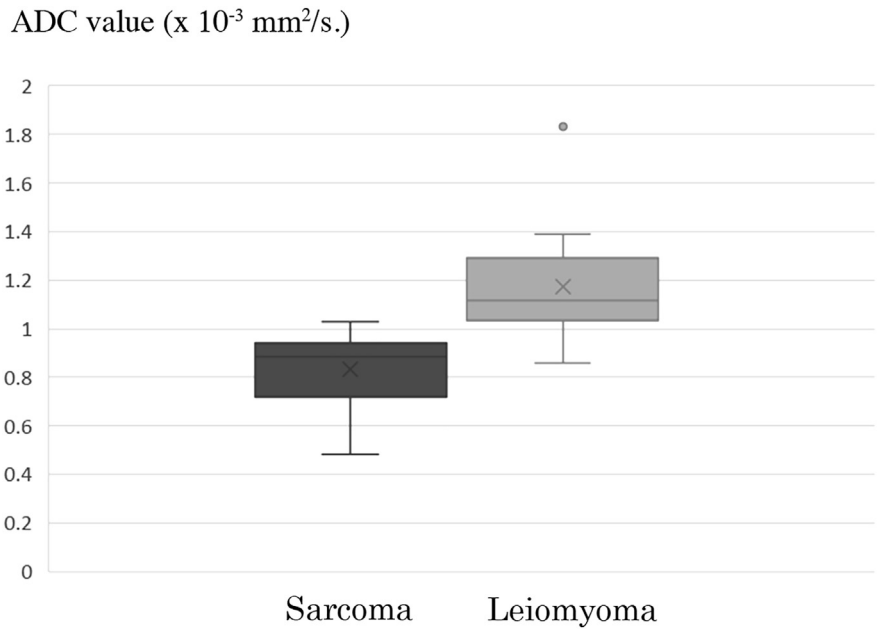

Fig. 5. Box-and-whiskers plots of ADCs of sarcomas and benign leiomyomas.

endometriosis by demonstrating hemorrhage of varying chronicity [19]. In the current study, susceptibility-weighted MR sequences are sensitive for intra-tumoral hemorrhage in patients with sarcomas, and considered as a useful sequence for the diagnosis of uterine sarcoma as high-grade malignant tumor with hemorrhagic necrosis.

Leiomyomas are the most common benign uterine neoplasm and are composed of smooth muscle and fibrous connective tissue. Leiomyomas may outgrow their blood supply as they enlarge, resulting in various types of degeneration [7]. However, hemorrhage and necrosis are not common (other than red degeneration) in benign leiomyomas [20]. In the current study, only one of 24 benign leiomyomas showed speckled intra-tumoral hemorrhage on susceptibility-weighted MR sequences. The leiomyoma with hemorrhage was histologically diagnosed as cellular leiomyoma, which could contain focal hemorrhagic foci [20]. The other 23 usual leiomyomas with or without degeneration did not show intra-tumoral hemorrhage both on T1-weighted images or on susceptibility-weighted MR sequences.

High signal intensity on DWI is suggestive for uterine sarcomas, however, some benign leiomyomas may also show high signal intensity [14,15,17]. In the current study, all 10 sarcomas and 3 leiomyomas showed high signal intensity on DWI. Relative high cellularity (cellular leiomyoma), or T2 shine-through effect due to edema or degeneration may cause signal increase of benign leiomyomas on DWI ($b = 800–1000\ s/mm^2$), and the lack of hemorrhage on susceptibility-weighted MR sequences may be suggestive for benign leiomyomas.

The retrospective nature and small population (only patients who had undergone SWAN were included) are limitations in this study. Further studies in larger populations to verify the results are needed. It is also a limitation that only one leiomyoma variant (cellular leiomyoma) was included in this study. It may make sense that only one cellular leiomyoma was included in randomly selected 24 benign leiomyomas because of the rarity of leiomyoma variants (about 1 in 100 cases), however, imaging differentiation between sarcoma and leiomyoma is important for leiomyoma variants which can have atypical DWI/ADC and T2 features [14,15,18]. It will be important to evaluate the performance of susceptibility-weighted MR sequences in differentiating such leiomyoma variants from sarcoma in the future. Leiomyoma with red degeneration was not included in the current study, and which may be another limitation. Because red degeneration is caused by hemorrhagic infarction, signal voids reflecting hemorrhage may be observed on susceptibility-weighted MR sequences. However, leiomyoma with red degeneration usually shows diffuse high signal intensity or peripheral high intensity rim on T1-weighted images, and could be differentiated from sarcomas.

Susceptibility-weighted MR sequences such as SWAN are sensitive MR technique which demonstrate intra-tumoral hemorrhage of uterine sarcomas, and we conclude that the demonstration of intra-tumoral hemorrhage in patients suspected with uterine sarcomas by susceptibility-weighted MR sequences may provide valuable diagnostic findings.

References

[1] Santos P, Cunha TM. Uterine sarcomas: clinical presentation and MRI features. Diagn Interv Radiol 2015;21:4–9.
[2] Sahdev A, Sohaib SA, Jacobs I, Shepherd JH, Oram DH, Reznek RH. MR imaging of uterine sarcomas. AJR 2001;177:1307–11.
[3] Cornfeld D, Israel G, Martel M, Weinreb J, Schwartz P, McCarthy S. MRI appearance of mesenchymal tumors of the uterus. Eur J Radiol 2010;74:241–9.
[4] Tanaka YO, Nishida M, Tsunoda H, Okamoto Y, Yoshikawa H. Smooth muscle tumors of uncertain malignant potential and leiomyosarcomas of the uterus: MR findings. J Magn Reson Imaging 2004;20:998–1007.
[5] Tanaka YO, Tsunoda H, Minami R, Yoshikawa H, Minami M. Carcinosarcoma of the uterus: MR findings. J Magn Reson Imaging 2008;28:434–9.
[6] Takeuchi M, Matsuzaki K, Harada M. Carcinosarcoma of the uterus: MRI findings including diffusion-weighted imaging and MR spectroscopy. Acta Radiol 2016;57:1277–84.
[7] Murase E, Siegelman ES, Outwater EK, Perez-Jaffe LA, Tureck RW. Uterine leiomyomas: histopathologic features, MR imaging findings, differential diagnosis, and treatment. Radiographics 1999;19:1179–97.
[8] Dooms GC, Uske A, Brant-Zawadzki M, Kucharczyk W, Lemme-Plaghos L, Newton TH, et al. Spin-echo MR imaging of intracranial haemorrhage. Neuroradiology 1986;28:132–8.
[9] Bradley Jr. WG. MR appearance of hemorrhage in the brain. Radiology 1993;189:15–26.
[10] Haacke EM, Xu Y, Cheng YC, Reichenbach JR. Susceptibility weighted imaging (SWI). Magn Reson Med 2004;52:612–8.
[11] Boeckh-Behrens T, Lutz J, Lummel N, Burke M, Wesemann T, Schöpf V, et al. Susceptibility-weighted angiography (SWAN) of cerebral veins and arteries compared to TOF-MRA. Eur J Radiol 2012;81:1238–45.
[12] Sehgal V, Delproposto Z, Haddar D, Haacke EM, Sloan AE, Zamorano LJ, et al. Susceptibility-weighted imaging to visualize blood products and improve tumor contrast in the study of brain masses. J Magn Reson Imaging 2006;24:41–51.
[13] Löbel U, Sedlacik J, Sabin ND, Kocak M, Broniscer A, Hillenbrand CM, et al. Three-dimensional susceptibility-weighted imaging and two-dimensional T2*-weighted gradient-echo imaging of intratumoral hemorrhages in pediatric diffuse intrinsic pontine glioma. Neuroradiology 2010;52:1167–77.
[14] Tamai K, Koyama T, Saga T, Morisawa N, Fujimoto K, Mikami Y, et al. The utility of diffusion-weighted MR imaging for differentiating uterine sarcomas from benign

leiomyomas. Eur Radiol 2008;18:723–30.
[15] Takeuchi M, Matsuzaki K, Nishitani H. Hyperintense uterine myometrial masses on T2-weighted magnetic resonance imaging: differentiation with diffusion-weighted magnetic resonance imaging. J Comput Assist Tomogr 2009;33:834–7.
[16] Namimoto T, Yamashita Y, Awai K, Nakaura T, Yanaga Y, Hirai T, et al. Combined use of T2-weighted and diffusion-weighted 3-T MR imaging for differentiating uterine sarcomas from benign leiomyomas. Eur Radiol 2009;19:2756–64.
[17] Thomassin-Naggara I, Dechoux S, Bonneau C, Morel A, Rouzier R, Carette MF, et al. How to differentiate benign from malignant myometrial tumours using MR imaging. Eur Radiol 2013;23:2306–14.
[18] Arleo EK, Schwartz PE, Hui P, McCarthy S. Review of leiomyoma variants. AJR 2015;205:912–21.
[19] Takeuchi M, Matsuzaki K, Harada M. Susceptibility-weighted MRI of extra-ovarian endometriosis: preliminary results. Abdom Imaging 2015;40:2512–6.
[20] Ueda H, Togashi K, Konishi I, Kataoka ML, Koyama T, Fujiwara T, et al. Unusual appearances of uterine leiomyomas: MR imaging findings and their histopathologic backgrounds. Radiographics 1999;19:131–45.